Proceedings of the
47th IEEE Conference on Decision and Control
Cancun, Mexico, Dec. 9-11, 2008

Closed-Loop System Identification of LPV Input-Output Models - Application to an Arm-Driven Inverted Pendulum

Sudchai Boonto and Herbert Werner

Abstract— **In this paper we show the possibility to merge an MIMO LPV system identification with closed-loop output error identification algorithm. The purposed method is tested with an arm-driven inverted pendulum as an application. The experimental results shown a significant improvement of the LPV model over a linear time-invariant model with the same structure.**

I. INTRODUCTION

In many real applications involving nonlinear plants, *Linear Time Invariant* (LTI) models are not sufficient for high performance controller designs. In order to achieve good performance throughout a wide operating range, while still using linear techniques, one can employ techniques based on *Linear Parameter Varying* (LPV) systems, which have received considerable attention [13]. There has been much work reported in the literature that illustrates that LPV control can outperform LTI control, see e.g. [13], [5], [4].

There are several methods to experimentally identify such LPV models. Two main direction can be distinguished. The first one is based state-space models, see [15], while the other is based on input-output models, see [3]. In this paper we consider the identification of LPV systems in input-output form as discussed in [3]. In this approach the model is parameterized such that the prediction error can be written in linear regression form. By using a quadratic cost function, the estimation problem becomes a least square problem. This method has been used in several practical applications [16], [4], [2]. On the other hand, most high performance controller design techniques are based on state space models; this is also true for LPV controller design. A transformation of input-output LPV models into state-space LPV models is therefore necessary, see [14].

In practice there are many situations in which identification in open loop is difficult or impossible, for example unstable plants and plants with integral behavior. Motivated by these practical considerations, closed-loop system identification methods have been used, developed and analyzed [11]. In recent years, many researchers recognize that identification in closed-loop provides certain advantages over open-loop identification [6].

In this work, we identify input-output LPV models in closed-loop, in order to obtain suitable models of unstable MIMO systems. For this purpose, we extend a closed-loop identification algorithm introduced by I. D. Landau and A. Karimi [7] to MIMO LPV systems. Moreover, a sufficient condition for stability and convergence of the algorithm is given.

The method is applied to an Arm-Driven Inverted Pendulum (ADIP) [12], [5], which is a single-input multiple-output (SIMO) system. This system is difficult to stabilize and control over a wide operating range. Since the system is unstable, initially a linear controller is used to stabilize a system in an initial range. A multi-sine signal [11] is then used as an excitation signal to excite all possible input-output levels of both outputs of the system.

This paper is organized as follows. In section II the model class considered here is defined. The closed-loop system identification approach used here is presented in section III. Section IV provides details of the experimental setup; experimental results are given in section V. Finally, conclusions are presented.

II. INPUT-OUTPUT LPV MODEL

We consider the following discrete-time input-output LPV model, as discussed in [16], [3].

$$A(q^{-1},p(k))y(k) = B(q^{-1},p(k))u(k-d) \tag{1}$$

where q^{-1} is the backward shift operator, $p(k) \in \mathbb{R}^q$ represents the scheduling variables, $y(k) \in \mathbb{R}^{ny\times 1}$ is the system output at time k, and $u(k) \in \mathbb{R}^{nu\times 1}$ is the system input. The polynomial matrices $A(q^{-1},p(k))$ and $B(q^{-1},p(k))$ are defined by

$$\begin{aligned} A(q^{-1},p(k)) &= I_{ny} + A_1(p(k))q^{-1} + \cdots + A_{na}(p(k))q^{-na} \\ B(q^{-1},p(k)) &= B_1(p(k))q^{-1} + \cdots + B_{nb}(p(k))q^{-nb} \end{aligned} \tag{2}$$

where $A_i \in \mathbb{R}^{ny\times ny}, B_i \in \mathbb{R}^{ny\times nu}$. The elements of the coefficient matrices A and B are functions of $p(k)$, which can be expressed as weighted sums of functions f_i of $p(k)$ in the following way

$$\rho_i(p(k)) = \rho_i^0 + f_1(p(k))\rho_i^1 + \cdots + f_{N-1}(p(k))\rho_i^{N-1} \tag{3}$$

where $\rho_i(p(k))$ represents either $A_i(p(k))$ or $B_i(p(k))$, $\{\rho_i^j, j = 1,2,\ldots,N-1\}$ are constant values, and $\{f_j(p(k)), j = 1,2,\ldots,N-1\}$ are functions of the online measurable variables $p(k)$.

The above system representation can be rewritten in linear regression form as

$$y(k) = \Theta\phi(k), \tag{4}$$

S. Boonto and H. Werner are with the Institute of Control Systems, Hamburg University of Technology , Eissendorfer Str. 40, 21073 Hamburg boonto@tu-harburg.deh.werner@tu-harburg.de

where the regressor vector is given by

$$\phi(k) = \varphi(k) \otimes \sigma(p(k)) \tag{5}$$

Here $\otimes$ is the Kronecker product and

$$\begin{aligned}\varphi^T(k) = [&-y^T(k-1) \ -y^T(k-2) \ \cdots \ -y^T(k-na) \\ &\cdots \ u^T(k-1) \ u^T(k-2) \ \cdots \ u^T(k-nb)] \\ \Theta = [&A_1^i \ A_2^i \ \cdots \ A_{na}^i \ B_1^i \ B_2^i \ \cdots \ B_{nb}^i] \\ \sigma(p(k)) = [&1 \ f_1(p(k)) \ \cdots \ f_{N-1}(p(k))]\end{aligned}$$

and $i = 1, \ldots, N-1$, $\sigma(p(k)) \in \mathbb{R}^{1\times N}$ and $\varphi^T(k) \in \mathbb{R}^{1\times(na+nb)}$.

A. Model Representation

The model of the system is written as

$$A(q^{-1}, p(k))\hat{y}(k) = q^{-d}B(q^{-1}, p(k))u(k) \tag{6}$$

which yields the predictor

$$\hat{y}(k+1, p(k)) = \hat{\Theta}\phi(k) \tag{7}$$

and with the prediction error

$$\begin{aligned}\varepsilon(k+1, p(k)) &= y(k+1) - \hat{y}(k+1, p(k)) \\ &= y(k) - \hat{\Theta}\phi(k).\end{aligned} \tag{8}$$

The advantage of rewriting the model in this linear form is not only that an open-loop recursive identification method can be used [3] but also that it enables closed-loop identification.

III. Identification in closed-loop

The closed-loop identification scheme used in this paper is based on *closed-loop output error* (CLOE) schemes [7]. The algorithm minimizes a quadratic criterion in terms of the CLOE, or drives the closed-loop output error to zero. It has been shown in [7], [8] that the method gives good results for the linear SISO cases. For MIMO LPV systems, one can substitute the LPV model in the algorithm by turning some scalar variables into matrix form.

A. Problem Formulation

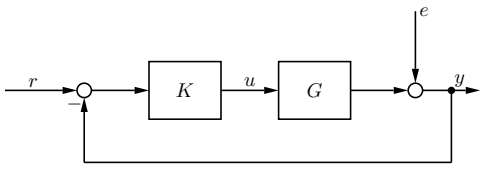

Fig. 1: Closed-loop system

Consider the MIMO system shown in Figure 1, where the plant model is given in input-output LPV form as in 1 by

$$A(q^{-1}, p(k))y(k) = B(q^{-1}, p(k))u(k-d) + e(k) \tag{9}$$

and

$$\begin{aligned}A(q^{-1}, p(k)) &= I_{ny} + A_1(p(k))q^{-1} + \cdots + A_{na}(p(k))q^{-na} \\ &= I_{ny} + q^{-1}A^*(q^{-1}, p(k))\end{aligned} \tag{10}$$

$$\begin{aligned}B(q^{-1}, p(k)) &= B(p(k))q^{-1} + \cdots + B_{nb}(p(k))q^{-nb} \\ &= q^{-1}B^*(q^{-1}, p(k))\end{aligned} \tag{11}$$

In Figure 1, $r(t) \in \mathbb{R}^{ny\times 1}$ is the external excitation, $e(t)$ corresponds to output disturbance. The nominal controller $K(q^{-1})$ is a controller designed based on an available nominal plant model. In the closed-loop system identification framework, this nominal controller is just required to stabilize the closed-loop in the required range of operation.

B. Closed-Loop Identification Schemes

In this paper, we consider the closed-loop output error with external excitation added to the controller input shown in Figure 2. This scheme is suitable for tracking and output disturbance rejection as described in [8]. The identification criterion in this case is

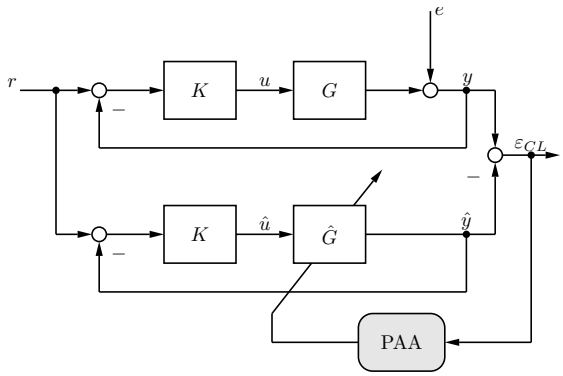

Fig. 2: Closed-loop identification scheme

$$\hat{\Theta}^* = \arg\min_{\theta} \|S_{yr}(q^{-1}) - \hat{S}_{yr}(q^{-1})\|_2 \tag{12}$$

where $S_{yr}(q^{-1})$ is the sensitivity function of the true system from $r(k)$ to $y(k)$ and $\hat{S}_{yr}(q^{-1})$ is the sensitivity of the predictor from $r(k)$ to $\hat{y}(k)$.

C. A Closed-loop Output Error Algorithms (CLOE)

The CLOE identification algorithms [7] is extended to MIMO LPV under the assumptions [6] that

- A1 the controller is an LTI controller;
- A2 the input-output part of the plant model belongs to the model set;
- A3 an external excitation is applied to the closed-loop system to identify a plant model.
- A4 the output disturbance is zero-mean white noise and independent of the external excitation signals.

In the case where the external excitation is the reference $r(k)$ as shown in Figure 2, the signal $u(k)$ is

$$u(k) = K(q^{-1})(r(k) - y(k)). \tag{13}$$

The adjustable closed-loop predictor is described by

$$\hat{y}^o(k+1) = \hat{\Theta}(k)\hat{\phi}(k) \qquad \textit{a priori} \tag{14}$$

$$\hat{y}(k+1) = \hat{\Theta}(k+1)\hat{\phi}(k) \qquad \textit{a posteriori} \tag{15}$$

$$\hat{\Theta}(k) = \begin{bmatrix} \hat{A}_1^i(k) & \dots & \hat{A}_{na}^i(k) & \hat{B}_1^i & \dots & \hat{B}_{nb}^i \end{bmatrix} \tag{16}$$

$$\hat{\phi}(k) = \psi(k) \otimes \sigma(p(k)) \tag{17}$$

$$\psi^T(k) = [-\hat{y}^T(k) \ \cdots \ -\hat{y}^T(k-na+1) \ \hat{u}^T(k) \ \cdots \ \hat{u}^T(k-nb+1)] \tag{18}$$

$$\hat{u}(k) = K(q^{-1})(r(k) - \hat{y}(k)) \tag{19}$$

where $\hat{y}^o(k+1)$ and $\hat{y}(k+1)$ represent the *a priori* and the *a posteriori* outputs of the closed-loop predictor, $\hat{u}(k)$ is the control signal delivered by the controller using the *a posteriori* output of the predictor and not the measured outputs.

For the case of a quasi-LPV model [1] $\sigma(p(k))$ is a vector of functions of either $\hat{y}(k)$ or $\hat{u}(k)$ while for the general LPV model $\sigma(p(k))$ is a vector function of any measured data.

The closed-loop prediction error is given by

$$\varepsilon_{CL}^o(k+1) = y(k+1) - \hat{y}^o(k+1) \qquad \textit{a priori} \tag{20}$$

$$\varepsilon_{CL}(k+1) = y(k+1) - \hat{y}(k+1) \qquad \textit{a posteriori} \tag{21}$$

In order to estimate the parameters of the plant, the parameter adaptation algorithm (PAA) for MIMO LPV is given by

$$\hat{\Theta}(k+1) = \hat{\Theta}(k) + \varepsilon_{CL}(k+1)\hat{\phi}^T(k)F(k) \tag{22}$$

$$F^{-1}(k+1) = \lambda_1(k)F^{-1}(k) + \lambda_2(k)\hat{\phi}(k)\hat{\phi}^T(k), \tag{23}$$

$$0 < \lambda_1(k) \le 1, \ 0 \le \lambda_2(k) < 2,$$

$$F(0) > 0, \ F^{-1}(k) > \alpha F^{-1}(0), \ 0 < \alpha < \infty,$$

$$F(k+1) = \frac{1}{\lambda_1(k)}\left[F(k) - \frac{F(k)\hat{\phi}(k)\hat{\phi}^T(k)F(k)}{\frac{\lambda_1(k)}{\lambda_2(k)} + \hat{\phi}^T(k)F(k)\hat{\phi}(k)}\right] \tag{24}$$

$$\varepsilon_{CL}(k+1) = \frac{\varepsilon_{CL}^o(k+1)}{1 + \hat{\phi}^T(k)F(k)\hat{\phi}(k)} \tag{25}$$

Here $\lambda_1(k)$ and $\lambda_2(k)$ are weighting sequences for the gain adaptation. A proof of (25) is given in appendix A. Equation (25) can also be written as

$$\varepsilon_{CL}(k+1) = P^{-1}(q^{-1}, p(k))(\Theta - \hat{\Theta}(k+1))\hat{\phi}(k) \tag{26}$$

where $P(q^{-1}, p(k)) = A(q^{-1}, p(k)) + q^{-d}B(q^{-1}, p(k))$. A proof of (26) is given in appendix B.

D. Stability Analysis for MIMO LPV Case

Given measurements of $r(k)$, $y(k)$ at time k, sequences of the regression vector $\hat{\phi}(k)$ and the estimate $\hat{\Theta}(k)$ can be easily constructed using the CLOE algorithm. Then we have the following result.

***Theorem** 3.1:* Consider the plant (9) satisfying assumptions A1-A4 and the parameter estimation algorithm (22)-(25). If the transfer function

$$H(q^{-1}, p(k)) = P^{-1}(q^{-1}, p(k)) - \frac{\lambda}{2}I \tag{27}$$

is strictly positive real for $\max_k \lambda_2(k) \le \lambda < 2$ and $P(q^{-1}, p(k)) = A(q^{-1}, p(k)) + q^{-d}B(q^{-1}, p(k))$ then

(i) There exists a finite random matrix $\tilde{\Theta}$ (not necessarily equal to Θ) such that

$$\lim_{k\to\infty} \hat{\Theta}(k) = \tilde{\Theta} \tag{28}$$

(ii) $\lim_{N\to\infty} \sup \frac{1}{N}\sum_{k=1}^{N} \|(\tilde{\Theta}(k+1) - \Theta)\hat{\theta}(k)\|^2 < \infty,$

Proof: The proof is similar to the LTI case see [17]. ■

IV. Application to the Arm-Driven Inverted Pendulum (ADIP)

The arm-driven inverted pendulum (ADIP) has been used to test the performance of LPV control by Kajiwara and others in [5]. A laboratory version of this plant is produced by Quanser Inc. [12]. The ADIP is shown in Figure 3. The

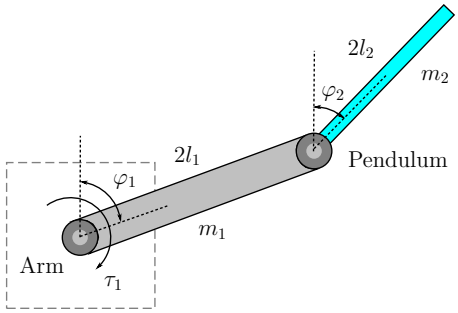

Fig. 3: Arm-Driven Inverted Pendulum (ADIP)

pendulum is the top link, it is hinging on the rotated arm - the bottom link - which is driven by a DC motor. The plant input is the voltage applied to the motor that drives the arm; controlled outputs are the angular position φ_1 of the arm, and the position of the pendulum φ_2 which is to be held at 0. When a wide range of values of the angle φ_1 is considered, an LTI model is not sufficient for controller design.

In this section, the system will be identified in MIMO LPV form by using the method described before. An LTI controller will be designed first to stabilize the system in an initial range, and input-output data will be collected.

A. Experiment Setup

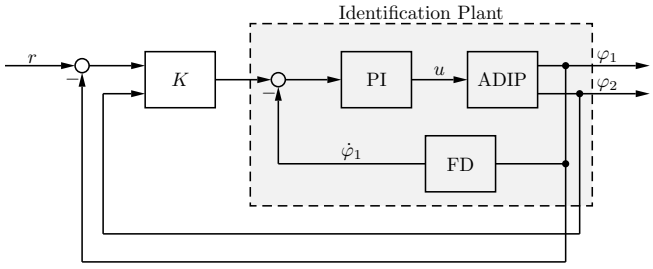

Fig. 4: Overall ADIP system for closed-loop identification

The closed-loop configuration is shown in Figure 4, where K is a stabilizing LTI $\mathcal{H}_\infty$ controller based on a nominal

model supported by Quanser [12], and an inner PI loop is used to control the angular velocity of the arm. Since the angular velocity $\dot{\varphi}_1$ cannot be directly measured, a differentiator filter FD is used to determine the angular velocity of the arm from its angular position φ_1. The PI controller and the filter FD are considered as part of the plant – the system to be identified is shown in the dashed box in Figure 4.

The first controller designed with 5 ms sampling time stabilizes the system in a range of φ_1 up to $\pm 50°$. However, this sampling time turned out to be too fast for system identification. A multi-level pseudo-random signal (MLPRBS) was used as a reference signal and the shortest rise time of both outputs φ_1 and φ_2 was measured. The fastest rise time is about 0.5 second, and a sampling time of 10 ms was chosen for identification. With this sampling time , the discrete-time $\mathcal{H}_\infty$ Controller is redesigned to stabilize the system in the same range.

B. Excitation Signal Design

An important step in MIMO LPV system identification is the excitation signal design. For the recursive system identification described in the previous section a *persistency of excitation* condition has to be satisfied in order to guarantee the convergence of the algorithm [3], [16].

In practice, the following multi-sine signal with sufficient harmonics can be used to guarantee this condition [11]

$$u(k) = \lambda \sum_{i=1}^{N_s/2} \sqrt{2\alpha_i}\cos(\omega_i kT + \phi_i) \tag{29}$$

where $\omega_i = 2\pi i/N_s T$. The power spectrum of this multi-sine signal can be directly specified by the user through the selection of the scaling factor λ, the Fourier coefficients α_i, the number of harmonics n_s the signal length N_s, and the sampling time T. More details can be found in [10].

The outputs φ_1 and φ_2 have different frequency bands and amplitudes (not shown here). The excitation signal should cover both bands but with different amplitudes in each frequency band. In this case

$$u(k) = \lambda_1 \sum_{i=1}^{N_s/2} \sqrt{2\alpha_i}\cos(\omega_i kT + \phi_i) + \lambda_2 \sum_{j=1}^{N_s/2} \sqrt{2\alpha_j}\cos(\omega_j kT + \phi_i). \tag{30}$$

Following the guidelines in [10], α_g is chosen as

$$\alpha_g = \begin{cases} 1, & g = 1, \ldots, n_s \\ hf, & g = n_s + 1, \ldots, N_s/2 \end{cases} \tag{31}$$

where $g = i$ and j, and hf is the high frequency coefficient magnitude.

According to the power spectrum shown in Figure 5, the multi-sine input is composed of $u_1(k)$ which has 20 harmonics between 0.063 rad/sec and 3.77 rad/sec, and $u_2(k)$ which has 20 harmonics between 3.77 rad/sec and 37 rad/sec.

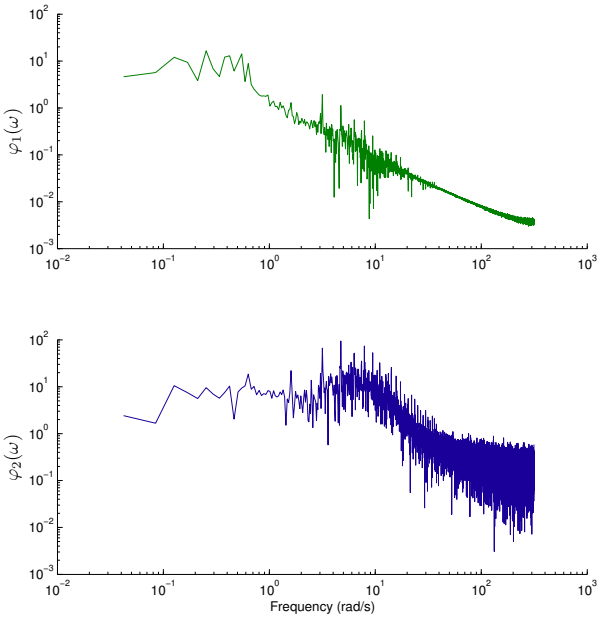

Fig. 5: Spectrum of both normalized outputs of ADIP: upper for φ_1, lower for φ_2.

The amplitude of $u_2(k)$ is half of $u_1(k)$ because this signal is aimed to excite the angle φ_2, which is more sensitive than φ_1, and this angle should not move far away from the $0°$ vertical position.

V. Experimental results

The ADIP is excited by the input signals explained above. The signal is periodic with 2 periods and 20400 samples. The identification method is applied to both linear and LPV model. Both models have a lag space $na = 4$ for past outputs and $nb = 4$ for past inputs. The delay time between input and output is set to 1 sample. The scheduling function of the LPV system is given by

$$\sigma(p(k)) = \begin{bmatrix} 1 & \sin(\varphi_1(k)) & \sin^2(\varphi_1(k)) \end{bmatrix}, \tag{32}$$

where $p(k) = \varphi_1(k)$.

Since the ADIP is a single-input two-output system, for the matrices we have $A_i \in \mathbb{R}^{2\times 6}$, $B_i \in \mathbb{R}^{2\times 3}$ and $i = 1, \ldots, 4$. The estimated matrices are given below where f_i refers to the i^{th} entry of $\sigma(p(k))$.

$$A_1 = \begin{bmatrix} -1.5220 & 0.0547 f_1 & 0.7961 f_2 & -0.0135 & -0.5240 f_1 & -0.2403 f_2 \\ -0.1441 & -1.3457 f_1 & 0.6388 f_2 & 0.2259 & -0.5907 f_1 & -0.1882 f_2 \end{bmatrix}$$

$$A_2 = \begin{bmatrix} 0 & 0.0415 f_1 & 0 & 0.0508 & 0.0708 f_1 & -0.2370 f_2 \\ 0 & -0.0197 f_1 & 0 & -0.6102 & 0.2006 f_1 & -0.2829 f_2 \end{bmatrix}$$

$$A_3 = \begin{bmatrix} -0.1774 & 0.0367 f_1 & -0.0048 f_2 & 0 & 0.0105 f_1 & 0 \\ -0.9106 & 0.1842 f_1 & -0.0898 f_2 & 0 & 0.0859 f_1 & 0 \end{bmatrix}$$

$$A_4 = \begin{bmatrix} 0.4454 & 0.2677 f_1 & -0.0435 f_2 & -0.7321 & -0.0764 f_1 & -0.0190 f_2 \\ 0.2922 & -2.0274 f_1 & -1.1781 f_2 & 0.6004 & 0.4825 f_1 & 0.0473 f_2 \end{bmatrix}$$

$$B_1 = \begin{bmatrix} 0.2511 & 0.1885f_1 & -0.0507f_2 \\ 0.0915 & 0.3491f_1 & 0.0243f_2 \end{bmatrix}$$
$$B_2 = \begin{bmatrix} -0.0897 & 0.3668f_1 & -0.0130f_2 \\ -0.2039 & 1.2420f_1 & -0.1622f_2 \end{bmatrix}$$
$$B_3 = \begin{bmatrix} 0.2832 & -0.3236f_1 & 0.1809f_2 \\ -1.7177 & 0.4875f_1 & 3.2041f_2 \end{bmatrix} \; B_4 = \begin{bmatrix} 0 & -0.0293f_1 & 0 \\ 0 & 0.0868f_1 & 0 \end{bmatrix}.$$

The convergence of the algorithm can be seen from the plot of parameter estimates shown in Figure 6. To validate the

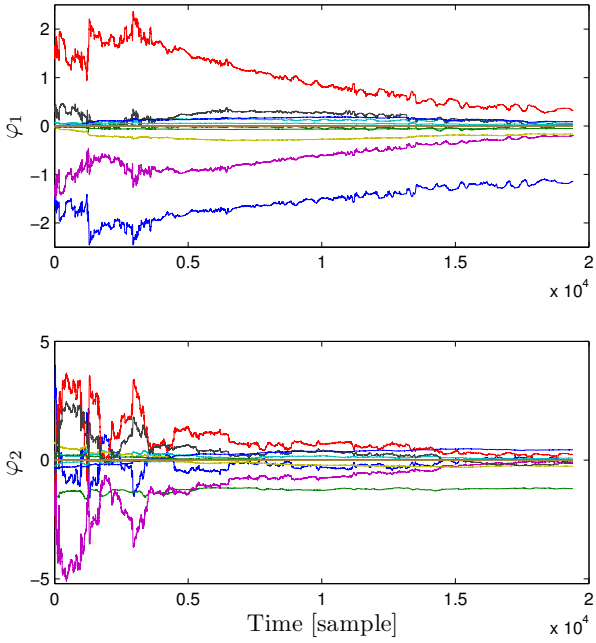

Fig. 6: Estimated parameters for φ_1 and φ_2.

resulting model, the measured response of the true closed-loop system is compared with the model simulation. In Figures 7 and 8 the comparison between the measured validation data and the simulation results of the LPV model is shown (the data have been scaled by the maximum value of each data set). It is easily seen from the figures that the LPV model gives better results than the linear model.

VI. CONCLUSIONS

In this paper the experimental identification of input-output LPV MIMO models in closed-loop has been considered. The proposed method has been experimentally validated on the ADIP system and provided satisfactory results.

VII. ACKNOWLEDGMENTS

The first author would like to thank Dr. A. Karimi for his suggestions.

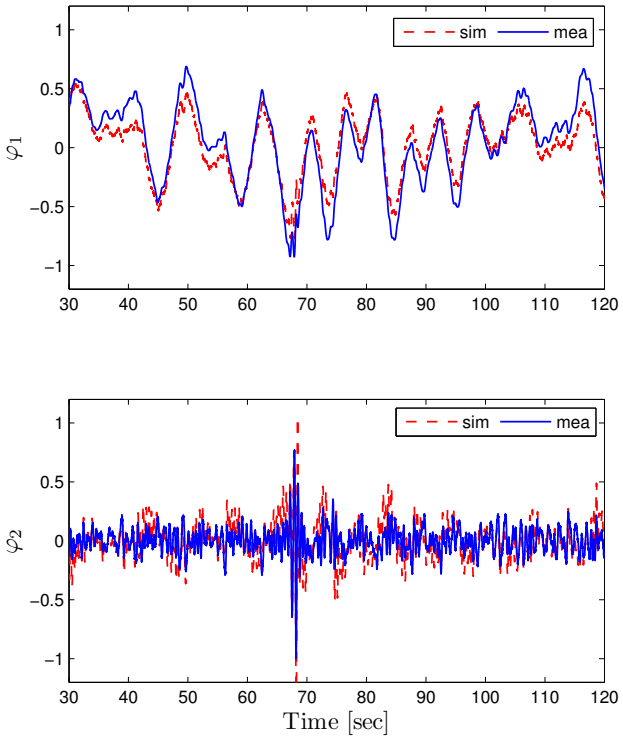

Fig. 7: Comparison between simulation result of linear model and measured data

APPENDIX

A. *Proof of* (25)

This proof is the MIMO extension version of the SISO case in [9].

$$\begin{aligned} \varepsilon_{CL}(k+1) &= y(k+1) - \hat{\Theta}(k+1)\hat{\phi}(k) \\ &= y(k+1) - \hat{\Theta}(k)\hat{\phi}(k) - [\hat{\Theta}(k+1) \\ &\quad - \hat{\Theta}(k)]\hat{\phi}(k) \end{aligned}$$

From (22), we get

$$\begin{aligned} \varepsilon_{CL}(k+1) &= \varepsilon^o_{CL}(k+1) \\ &\quad - \varepsilon_{CL}(k+1)\hat{\phi}^T(k)F(k)\hat{\phi}(k) \\ &= \frac{\varepsilon^o_{CL}(k+1)}{1+\hat{\phi}^T(k)F(k)\hat{\phi}(k)} \end{aligned}$$

B. *Proof of* (26)

From the system (9), for simplicity q^{-1} and $p(k)$ are omitted,

$$\begin{aligned} y(k+1) &= -A^*y(k) + B^*u(k-d) + e(k+1) \\ &= -A^*y(k) + q^{-d}B^*(-Ky(k) + Kr(k)) \\ &\quad + e(k+1) \\ &= -(A^* + q^{-d}B * K)\varepsilon_{CL}(k) - A^*\hat{y}(k) \\ &\quad + q^{-d}B^*\hat{u} + e(k+1) \\ &= \Theta\hat{\phi(k)} - (A^* + q^{-d}B^*K)\varepsilon_{CL}(k) + e(k+1). \end{aligned}$$

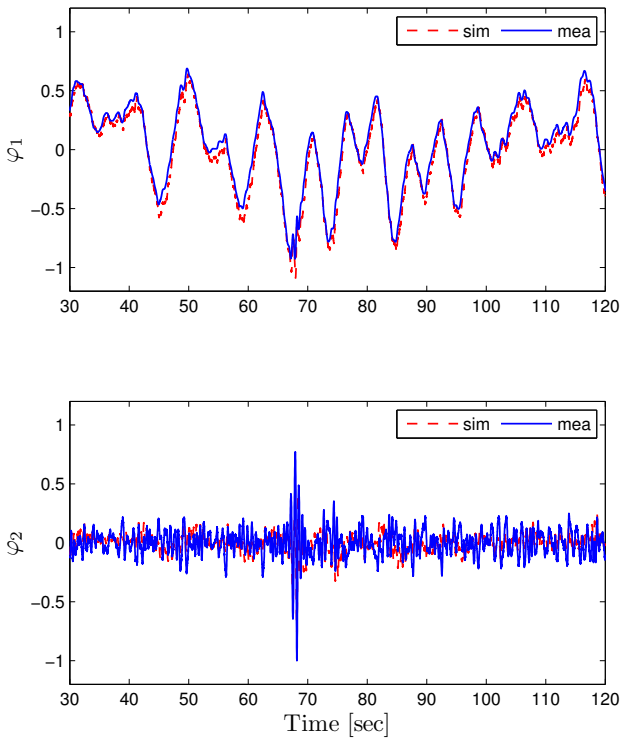

Fig. 8: Comparison between simulation result of LPV model and measured data

Then,

$$\begin{aligned}\varepsilon_{CL}(k) &= (\Theta - \hat{\Theta})\phi(k) - (A^* + q^{-d}B^*K)\varepsilon_{CL}(k) \\ &= P^{-1}(\Theta - \hat{\Theta})\hat{\phi}(k) + P^{-1}e(k+1).\end{aligned}$$

where $P = I + q^{-1}(A^* + q^{-d}B^*K) = A + q^{-d}BK$.

References

[1] P. Apkarian, G. Becker, P. Gahinet, and H. Kajiwara. LMI techniques in control engineering from theory to practice. In *Workshop Notes - IEEE Conference on Decision and Control*, Kobe, Japan, December 9-10 1996.

[2] R. T. Bambang and H. Subagiyo. LPV model identification of feed-gas pre-heater in ammonia plant. In *Proceedings of the 18th IASTED International Conference Modelling and Simulation*, pages 331–337, Montreal, Quebec, Canada, May 30–June 1 2007.

[3] B. Bamieh and L. Giarré. Identification of linear parameter varying models. *International Journal of Robust and Nonlinear Control*, 12(9):841–853, July 2002.

[4] L. Giarré, D. Bauso, P. Falugi, and B. Bamieh. LPV model identification for gain scheduling control: An application to rotating stall and surge control problem. *Control Engineering Practice*, 14(4):351–361, 2006.

[5] H. Kajiwara, P. Apkarian, and P. Gahinet. LPV techniques for control of an inverted pendulum. *IEEE Control Systems Magazine*, 19(1):44–54, February 1999.

[6] I. D. Landau. Identification in closed loop: A powerful design tool (better design models, simpler controllers). *Control Engineering Practice*, 9(1):51–65, 2001.

[7] I. D. Landau and A. Karimi. Recursive algorithms for identification in closed loop: A unified approach and evaluation. *Automatica*, 33(8):1499–1523, 1997.

[8] I. D. Landau and A. Karimi. A unified approach to model estimation and controller reduction (duality and coherence). *European Journal of Control*, 8(6):561–572, 2001.

[9] I. D. Landau and G. Zito. *Digital Control Systems Design, Identification and Implementation*. Springer, 2006.

[10] H. Lee. *A Plant-Friendly Multivariable System Identification Framework based on Identification Test Monitoring*. PhD thesis, Arizona State University, 2006.

[11] L. Ljung. *System Identification Theory for the User*. Prentice Hall, Upper Saddle River, NJ, 2 edition, 1999.

[12] Quanser Consulting Inc. *SRV03 Direct Drive Rotary Plant with Slipring: Position Servo & Planar Self-Erecting IP*.

[13] W. J. Rugh and J. S. Shamma. Research on gain scheduling. *Automatica*, 36(10 10 10):1401–1425, 2000.

[14] R. Tóth, F. Felici, P. S. C. Heuberger, and P. M. J. Van den Hof. Discrete time LPV I/O and state space representations, differences of behavior and pitfalls of interpolation. In *Proceedings of the European Control Conference*, pages 5418–5425, Kos, Greece, July 2–5 2007.

[15] V. Verdult. *Nonlinear System Identification: A State-space Approach*. PhD thesis, University of Twente, The Netherlands, 2002.

[16] X. Wei. *Advanced LPV Techniques for Diesel Engines*. PhD thesis, Joannes Kepler Universität, Linz, Austria, 2006.

[17] W.-S. Yu. An indirect adaptive pole-placement control for MIMO discrete-time stochastic systems. *International Journal of Adaptive Control and Signal Processing*, 19(7):547–573, 2005.